Damian Wierzbicki - Kamil Krasuski

DETERMINING THE ELEMENTS OF EXTERIOR ORIENTATION IN AERIAL TRIANGULATION PROCESSING USING UAV TECHNOLOGY

Unmanned Aerial Vehicles (UAVs) are still an interesting and current research topic in photogrammetry. An important issue in this area is determining the elements of exterior orientation of image data acquired at low altitudes. The article presents selected mathematical methods (TGC, TIC, TAD) of estimating elements of exterior orientation for image data obtained at low altitudes. The measurement data for the experimental test were recorded by the Unmanned Aerial Vehicle platform Trimble UX-5. In the framework of the test photogrammetric flight, the authors obtained 506 images and navigation data specifying the position and orientation of the Unmanned Aerial Vehicle. As a result of the research, it is proven possible to show the usefulness of the mathematical models (TGC, TIC, TAD) in estimation of elements of exterior orientation.

Keywords: *GNSS, INS, UAV, digital aerial triangulation, elements of exterior orientation, aerial photogrammetry*

1 Introduction

Development of the UAV technology made it possible to acquire image data o at low altitudes, as well. Georeferencing of image data taken by the Unmanned Aerial Vehicle (UAV) is performed in the process of digital aerial triangulation [1-2]. Within the classical process of digital aerial triangulation, the elements of exterior orientation and also coordinates of the measured ground control points, are taken. In the case of elements of exterior orientation, the coordinates of the centre of projection are determined for each image, referenced to the ground layout and the deflection angles of the camera referenced to the photogrammetric camera system. The typical accuracy of determining the elements of exterior orientation in the process of digital aerial triangulation for linear elements is approximately at a level of 0.1 m, and for angle elements, is respectively higher than 0.1^0. The approximate values of exterior orientation may be determined based on measurements of the GNSS/INS sensors, mounted on an UAV platform [3-4]. The basic navigation equipment of an UAV should contain at least a GNSS single-frequency code receiver and additionally a measurement system of gyroscopes and accelerometers for the needs of the INS system operation. The GNSS satellite receiver primarily facilitates determining the position of an Unmanned Aerial Aircraft in the three dimensional Cartesian coordinate XYZ. It also allows determining the heading and airspeed of an Unmanned Aerial Vehicle [5-7]. The above-mentioned navigation parameters of the GNSS receiver are determined in near real-time by an UAV control system and stored in the device's memory at a specified time interval. The measurement system of the INS sensor recovers the YPR (Yaw, Pitch and Roll) values of rotation angles on the basis of the movement of the gyroscopes and specifying the acceleration value from the accelerometer sensors. The readings of the YPR angles indicate an UAV position in airspace, whereas the acceleration values make it possible to designate the aircraft relative position [8-11].

The navigation parameters from the GNSS receiver are usually referenced to the GPS system time and the INS measurement system may have a separate built-in time pattern to register the observed data. It must be stressed that the GNSS receiver determines the UAV position with the absolute positioning accuracy of up to 10 m, whereas the INS relative accuracy becomes considerably deteriorated during the measurements. Furthermore, the accuracy of recording the YPR rotation angles equals 5^0 for an UAV. In order to correct the designated navigation parameters for an UAV, it is necessary to use exterior mathematical models so as to smooth the obtained findings. One of the examples of the integration of GNSS/INS data is the implementation, in computing, the recursive Kalman filter, reducing and eliminating measurements that stand out from a set of recorded navigational data. In addition, Kalman filtering ensures increasing accuracy in determining the UAV accuracy during the experimental test [12-14].

For aerial photogrammetry, determining the coordinate values and rotation angles for an UAV is a key element in the process of determining the elements of exterior orientation. The designated position of an UAV using a GNSS sensor forms the basis for reconstructing the camera position at the moment of exposure. Besides, the YPR rotation angles are exploited in the process of transformation to determine the angle OPK (Omega, Phi, Kappa) elements

Damian Wierzbicki[1,*], Kamil Krasuski[2]
[1]Institute of Geodesy, Faculty of Civil Engineering and Geodesy, Military University of Technology, Warszawa, Poland
[2]Institute of Navigation, Military University of Aviation, Deblin, Poland
*E-mail of corresponding author: damian.wierzbicki@wat.edu.pl

in the photogrammetric camera layout. The approximate values of exterior orientation are a valuable research and information material for conducting the process of digital aerial triangulation, using the coordinates of ground control points (GCPs).

The aim of this paper is to present mathematical methods for establishing the approximate values of elements of exterior orientation and to verify the obtained results with regard to the final products of digital aerial triangulation. The measurement data for the experimental test come from a photogrammetric flight performed by the Trimble UX-5 rover in Tylicz.

2 Mathematical models for designation of the exterior orientation elements

The chapter describes the mathematical models for the determination of elements of exterior orientation with the on-board GNSS/INS data registered by an UAV and on the basis of the method of digital aerial triangulation.

2.1 Mathematical models for designation of the projection centre coordinates

A single-frequency GNSS receiver, mounted on a UAV platform, can be used to determine approximate coordinate values of the centre of projection. Coordinates of the centre of projection are determined in a two-step process, i.e. in the first stage a UAV position is determined and in the second stage the coordinates of the projection center of each image are designated, taking into account the correction of eccentricity between the position of the GNSS receiver antenna and the camera. The basic observation equation to determine a UAV position for the GNSS sensor can be expressed in the following manner [4]:

$$l = \rho + c\cdot(dtr - dts) + Trop + rel + ion + \\ + bias + M_l, \tag{1}$$

where:
l - measurement code C/A at L1 frequency,
r - geometric distance between the satellites GNSS and the receiver,
$\rho = \sqrt{(X_r - X_s)^2 + (Y_r - Y_s)^2 + (Z_r - Z_s)^2}$,
(X_r, Y_r, Z_r) - position of an unmanned aerial platform in the geocentric frame,
(X_s, Y_s, Z_s) - position of GNSS satellite in orbit,
c - speed of light,
dtr - receiver clock bias for GNSS observations,
dts - satellite clock bias for GNSS observations,
$Trop$ - tropospheric delay for GNSS observations,
Ion - ionospheric delay for GNSS observations,
Rel- relativistic effects for GNSS observations,
$bias$ - summary expression for hardware delay in the GNSS system,
M_l - multipath effect and measurement noise.

In Equation (1) the determined parameters are the aircraft coordinates, (X_r, Y_r, Z_r) referenced to the phase centre of the antenna receiver mounted on the UAV platform and the receiver clock bias dtr. The unknown parameters from Equation (1) are determined using the Kalman filtering in accordance with interval recording of an observation. The UAV coordinates are used to determine the coordinates of the projection center for each image, see below [13-14]:

$$\begin{bmatrix} X_{kr} \\ Y_{kr} \\ Z_{kr} \end{bmatrix} = \begin{bmatrix} X_r \\ Y_r \\ Z_r \end{bmatrix} + \begin{bmatrix} e_x \\ e_y \\ e_z \end{bmatrix}, \tag{2}$$

where:
(X_{kr}, Y_{kr}, Z_{kr}) - coordinate of the camera projection centre,
(e_x, e_y, e_z) - parameters of the camera eccentricity.

2.2 Mathematical models for designation of the exterior orientation angle elements

The INS sensor installed on a UAV platform ensures reconstruction of a UAV orientation in airspace by means of the YPR rotation angles. The values of YPR angles allow designating approximate angular elements of OPK exterior orientation based on the transformation between the INS sensor layout and the camera layout, as below [15]:

$$C_E^B = T_b^B \cdot \left(C_{n0}^{n'} \cdot C_e^{n0} \cdot (C_e^{ni})^T \cdot C_b^{ni} \right)^T \cdot (T_n^E)^T, \tag{3}$$

where:
C_E^B - orthogonal matrix, containing angular OPK elements,

$$C_E^B = \begin{bmatrix} \cos\varphi\cos\kappa & -\cos\varphi\sin\kappa & \sin\varphi \\ \cos\varpi\sin\kappa + \sin\varpi\sin\varphi\cos\kappa & \cos\varpi\cos\kappa - \sin\varpi\sin\varphi\sin\kappa & -\sin\varpi\cos\varphi \\ \sin\varpi\sin\kappa - \cos\varpi\sin\varphi\cos\kappa & \sin\varpi\cos\kappa + \cos\varpi\sin\varphi\cos\kappa & \cos\varpi\cos\varphi \end{bmatrix},$$

φ - Phi angle,
$\varphi = \arcsin C_E^B(1,3)$,
ϖ - Omega angle,

$$\varpi = -arctg\left(\frac{C_E^B(2,3)}{C_E^B(3,3)}\right),$$

κ - Kappa angle,

$$\kappa = -arctg\left(\frac{C_E^B(1,2)}{C_E^B(1,1)}\right),$$

$$T_b^B = \begin{bmatrix} -1 & 0 & 0 \\ 0 & 1 & 0 \\ 0 & 0 & -1 \end{bmatrix},$$

T_b^B - the determinant of the matrix is equal to 1,

$$C_{n0}^{n'} = \begin{bmatrix} 1 & 0 & 0 \\ 0 & 1 & 0 \\ 0 & 0 & 1 \end{bmatrix},$$

$C_{n0}^{n'}$ - unit matrix,

$$C_e^{n0} = \begin{bmatrix} -\sin B_0 \cdot \cos L_0 & -\sin B_0 \cdot \sin L_0 & \cos B_0 \\ -\sin L_0 & \cos L_0 & 0 \\ -\cos B_0 & -\cos B_0 \cdot \sin L_0 & -\sin B_0 \end{bmatrix},$$

$C_e^{n0} = f(B_0, L_0)$,

C_e^{n0} - matrix that contains UAV coordinates in the ellipsoidal system;

(B_0, L_0) - the UAV coordinates refer to the central point of the flight trajectory,

$$C_e^{ni} = \begin{bmatrix} -\sin B_i \cdot \cos L_i & -\sin B_i \cdot \sin L_i & \cos B_i \\ -\sin L_i & \cos L_i & 0 \\ -\cos B_i & -\cos B_i \cdot \sin L_i & -\sin B_i \end{bmatrix},$$

$C_e^{ni} = f(B_i, L_i)$,

C_e^{ni} - matrix that contains UAV coordinates in the ellipsoidal system;

(B_i, L_i) - UAV coordinates for each measurement epoch,

C_b^{ni} - orthogonal matrix, containing angular YPR elements,

$$C_b^{ni} = \begin{bmatrix} \cos\psi \cdot \cos\theta & \cos\psi \cdot \sin\theta \cdot \sin\phi - \sin\psi \cdot \cos\phi & \cos\psi \cdot \sin\theta \cdot \cos\phi + \sin\psi \cdot \sin\phi \\ \sin\psi \cdot \cos\theta & \sin\psi \cdot \sin\theta \cdot \sin\phi + \cos\psi \cdot \cos\phi & \sin\psi \cdot \sin\theta \cdot \cos\phi - \cos\psi \cdot \sin\phi \\ -\sin\theta & \cos\theta \cdot \sin\phi & \cos\theta \cdot \cos\phi \end{bmatrix}$$

ϕ - Roll angle,

θ - Pitch angle,

ψ - Yaw angle,

$$T_n^E = \begin{bmatrix} 0 & 1 & 0 \\ 1 & 0 & 0 \\ 0 & 0 & -1 \end{bmatrix},$$

T_n^E - the determinant of the matrix is equal to 1.

2.3 Mathematical models for designation of the exterior orientation elements using the digital aerial triangulation method

The method of digital aerial triangulation allows determining exterior orientation of elements with high accuracy: for linear elements of exterior orientation above 0.1 m and for elements of the angular exterior orientation above 0.1^0, respectively. The basic equation of digital aerial triangulation in the classic approach assumes the following form [16-17]:

(4)

$$\begin{cases} x_k - x_0 = \\ -f_k \left[\dfrac{r_{11}(X_T - X_{kr}) + r_{21}(Y_T - Y_{kr}) + r_{31}(Z_{T-Zkr})}{r_{13}(X_T - X_{kr}) + r_{23}(Y_T - Y_{kr}) + r_{33}(Z_{T-Zkr})} \right] \\ y_k - y_0 = \\ -f_k \left[\dfrac{r_{12}(X_T - X_{kr}) + r_{22}(Y_T - Y_{kr}) + r_{32}(Z_{T-Zkr})}{r_{13}(X_T - X_{kr}) + r_{23}(Y_T - Y_{kr}) + r_{33}(Z_{T-Zkr})} \right] \end{cases},$$

where:

(x_k, y_k) - image coordinates,

(x_0, y_0) - centre point of image coordinates,

f_k - focal length,

(X_T, Y_T, Z_T) - coordinates of ground control points in terrain frame,

(X_{kr}, Y_{kr}, Z_{kr}) - coordinates of the projection centre, expressed in terrain frame,

$$R = \begin{bmatrix} r_{11} & r_{21} & r_{31} \\ r_{12} & r_{22} & r_{32} \\ r_{13} & r_{23} & r_{33} \end{bmatrix},$$

- orthogonal matrix; matrix contains angle elements of exterior orientation,

$R = R(\varpi, \varphi, \kappa)$,

$(\varpi, \varphi, \kappa)$ - angle elements of exterior orientation.

3 Experimental test

In the framework of the experimental test, the exterior orientation elements were determined based on equations [2, 5-6, 18]. The navigation data to determine the elements of the exterior orientation from Equations (2) and (3) were recorded during the flight by the Trimble UX-5 unmanned aircraft system. The coordinate values of the platform Trimble UX-5 and YPR orientation angles are recorded by measurement instruments mounted on the platform and stored in the universal text format "log". The typical accuracy of the obtained coordinates of the Trimble UX-5 platform ranges from 5 m to 10 m and for the YPR orientation angles it is between 1^0 and 5^0, respectively [19]. The photogrammetric flight took place in Tylicz, in the south of Poland, in 2016. During the flight, 506 aerial images were taken, using a Sony NEX5R camera. All the aerial images were arranged in 22 rows (see Figure 1). The photogrammetric flight was executed at an altitude of 150 m, with an assumption that the average height of the terrain is approximately equal to 650 m.

Over the tested area, 10 ground control points and 5 independent check points were also measured for the needs of conducting digital aerial triangulation. The mutual orientation was performed based on an automatic measurement of tie points [16]. All of the measured points were signalled and their coordinates were designated by means of the GNSS RTK technique, with an accuracy no worse than 0.05 m. The process of digital aerial triangulation was carried out in the commercial UASMaster software. After conducting the process of digital aerial triangulation, the value of the mean error of typical observations equalled 5.4 μm (1.1 pixel). Moreover, the determined standard deviations for angle elements of the exterior orientation were over 0.043^0, whereas for the linear elements of exterior orientation they were higher than 0.1 m, accordingly. In addition, the RMS error at the control points equalled 0.21 m for the X coordinate, 0.04 m for the Y coordinate, and 0.11 m for the Z coordinate.

4 Results and discussion

For the sake of the executed experimental test, the elements of exterior orientation were determined based on the following research methods, which were defined by the authors as follows:

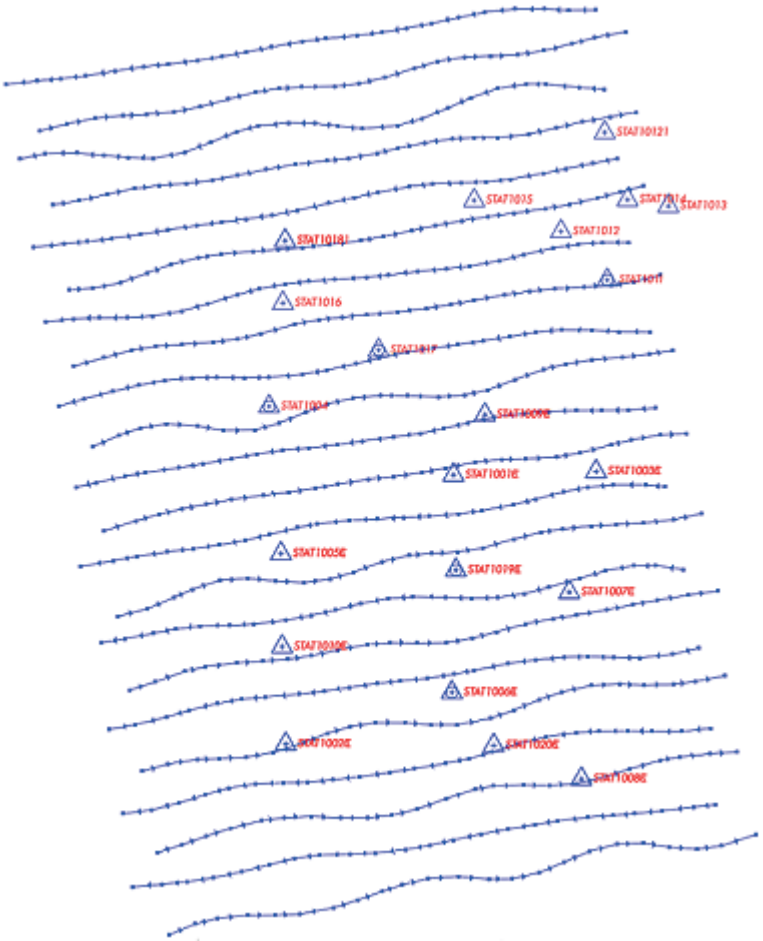

Figure 1 *Visualization of the test photogrammetric block - altitude 150 m*

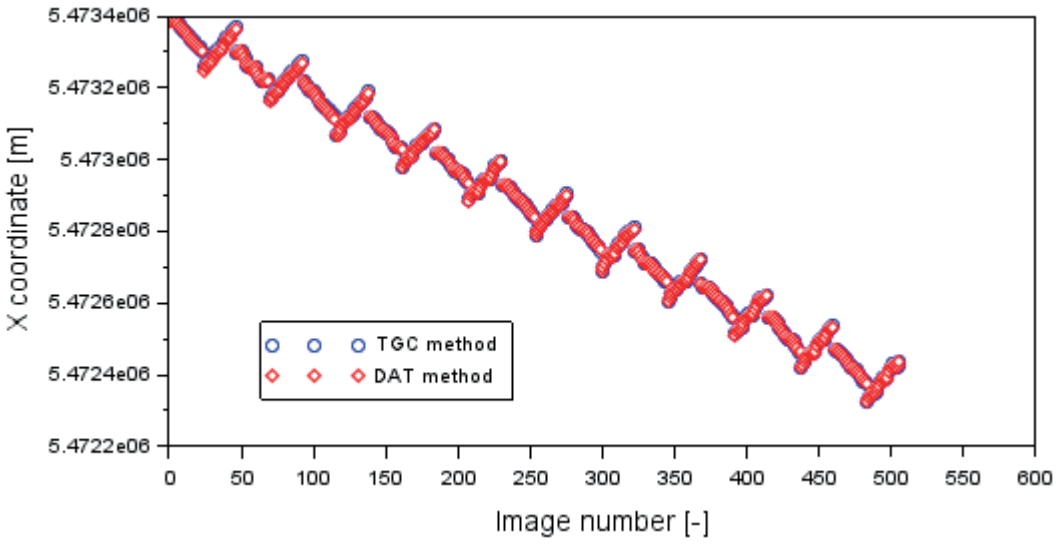

Figure 2 *Values of the projection centre X coordinate based on TGC and DAT methods*

- TGC method (**T**ranslation between **G**PS sensor and **C**amera sensor), the method relies on applying mathematical Equations (1) and (2),
- TGC method (**T**ranslation between **G**PS sensor and **C**amera sensor), the method relies on applying the mathematical model (3),
- DAT method (**D**igital **A**erial **T**riangulation processing), the method relies on applying the mathematical model (4).

Figures 2, 3 and 4 show values of the projection centre coordinates n along the X, Y and Z axes for the research methods TGC and DAT. The coordinates' values of the projection centre are referenced to the coordinate

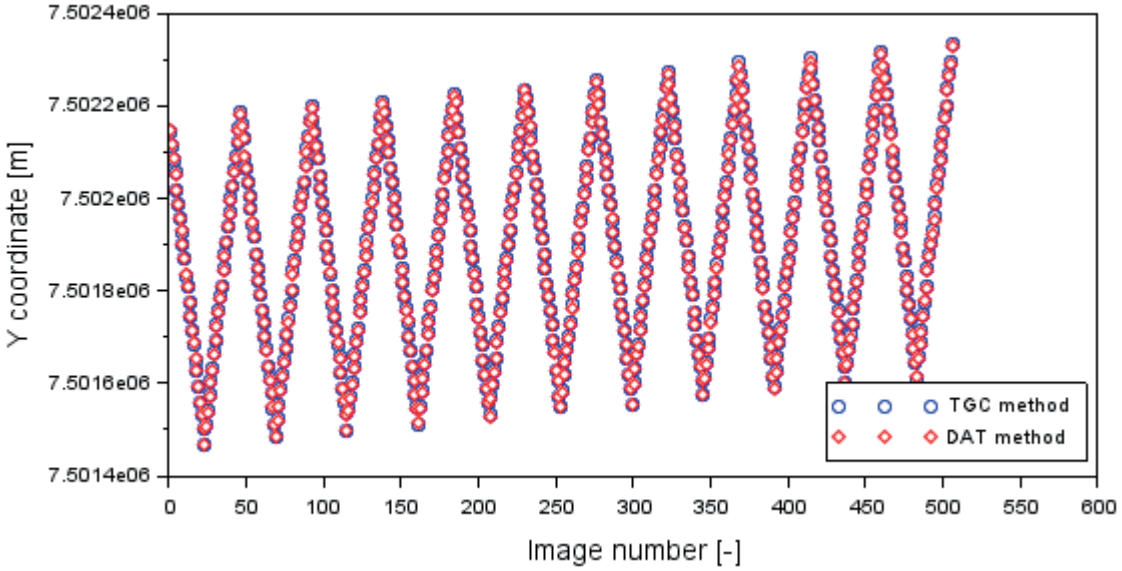

Figure 3 *Values of the projection centre Y coordinate based on TGC and DAT methods*

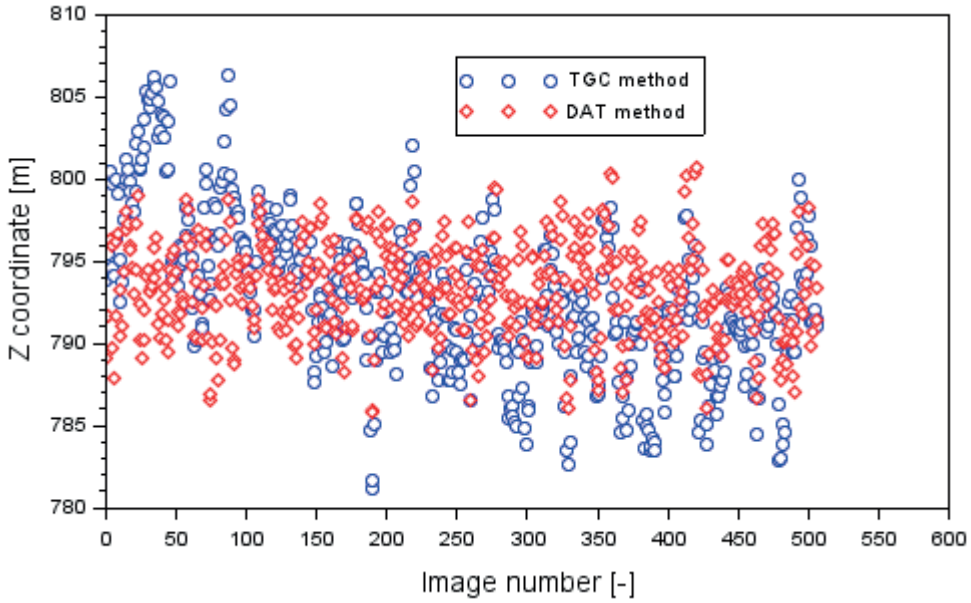

Figure 4 *Values of the projection centre Z coordinate of projection centre based on TGC and DAT methods*

system PUWG2000, zone 7. The X coordinate values in the TGC solution vary from 5472323.01 m to 5473391.36 m. In the DAT method, they change from 5472322.25 m to 5473389.66 m, accordingly. It should be stressed that the trajectory central point coordinates for the X axis are equal 5472869.82 m in the TGD method and 5472868.34 m in the TAD method, accordingly. The Y coordinate values in the TGC solution vary from 7501465.72 m to 7502332.94 m. In the DAT method, they change from 7501466.84 m to 7502331.47 m, respectively. The trajectory central point coordinates for the Y axis equal 7501900.01 m in the TGD method and 7501898.01 m in the TAD method, accordingly. The Z coordinate values in the TGC solution vary from 781.14 m to 806.26 m. In the DAT method, they change from 785.85 m to 800.67 m, respectively. The trajectory central point coordinates for the Z axis are equal 792.84 m in the TGD method and 793.21 m in the TAD method, accordingly.

Figures 5, 6 and 7 show the rotation element values of exterior orientation for the research methods TIC and DAT. Values of the Omega angle for the TIC solution change from -19.14^0 to 18.25^0, whereas in the DAT method they vary from -26.13^0 to 26.59^0, respectively. The average value of the Omega angle in the TIC method equals -0.060, and in the DAT method, it is 0.01^0, respectively. Values of the Phi angle for the TIC solution change from -15.64^0 to 14.32^0, whereas in the DAT method they vary from -9.80^0 to 13.17^0, respectively. The average value of the Phi angle in the TIC method equals 0.17^0, and in the DAT method, it is 0.50^0, respectively. Values of the Kappa angle in the TIC solution change from -179.88^0 to 25.91^0, whereas in the DAT method

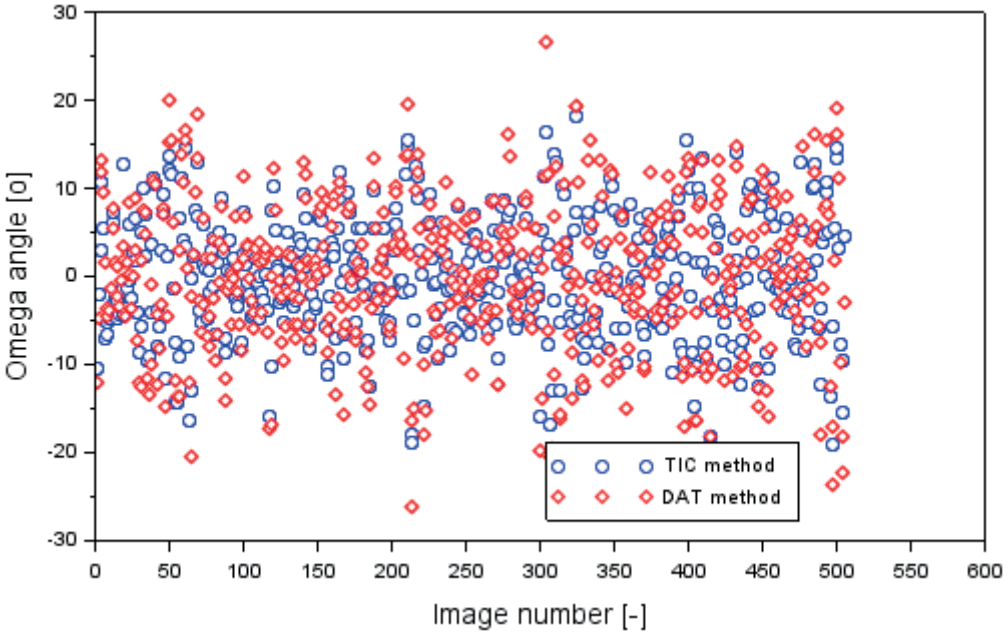

Figure 5 *Values of the Omega angle based on TIC and DAT methods*

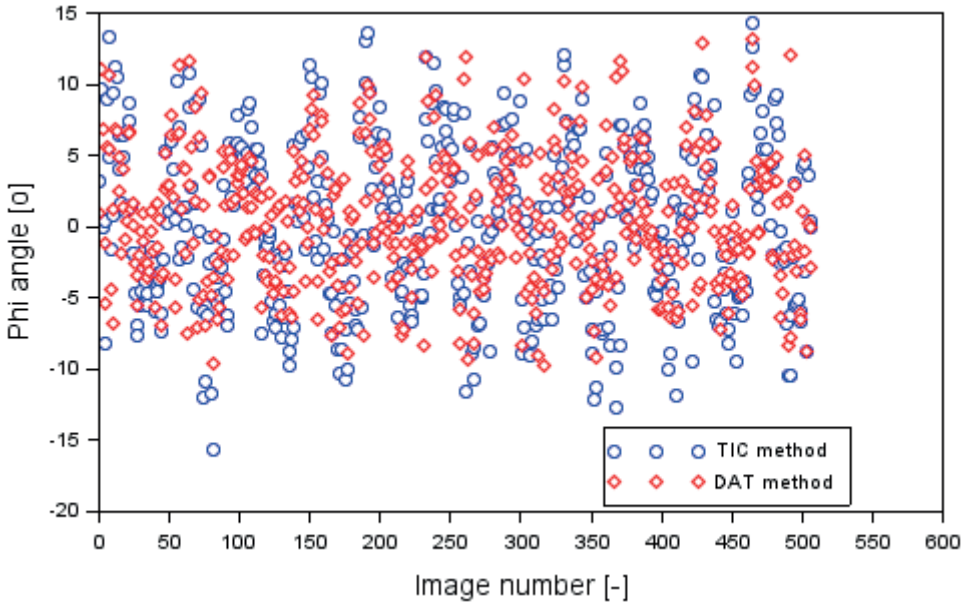

Figure 6 *Values of the Phi angle based on TIC and DAT methods*

they vary from -178.75^0 to 17.82^0, respectively. It should be noted that a large amplitude of results of the Kappa angle is caused by a change in direction of the flight of the Trimble UX-5 aircraft system from the west to the east or vice versa.

Figure 8 shows a difference in coordinate values of the centre of projection along the XYZ axis on the basis of the research methods TGC and DAT. The difference in coordinates of the centre of projection along the X, Y and Z axes were determined based on dependency [11]:

$$\begin{cases} dX = X_{kr}^{TGC} - X_{kr}^{DAT} \\ dY = Y_{kr}^{TGC} - Y_{kr}^{DAT} \\ dZ = Z_{kr}^{TGC} - Z_{kr}^{DAT} \end{cases}, \quad (5)$$

where:
$(X_{kr}^{TGC}, Y_{kr}^{TGC}, Z_{kr}^{TGC})$ - coordinates of the centre of projection in the TGC solution,
$(X_{kr}^{TAD}, Y_{kr}^{TAD}, Z_{kr}^{TAD})$ - coordinates of the centre of projection in the TAD solution.

The average value of the dX parameter equals 1.48 m with the scatter of results ranging from -2.72 m to 8.12 m. In addition, the standard deviation for parameter dX is 1.99 m, with the median being equal to 1.60 m. The average value of the dY parameter equals 1.99 m with the scatter of results between -2.89 m and 7.61. Furthermore, the standard deviation for parameter dY is 2.43 m, with the median being equal to 1.85 m. The average value of parameter dZ equals -0.38 m, with the scatter of results ranging from -8.51 m to

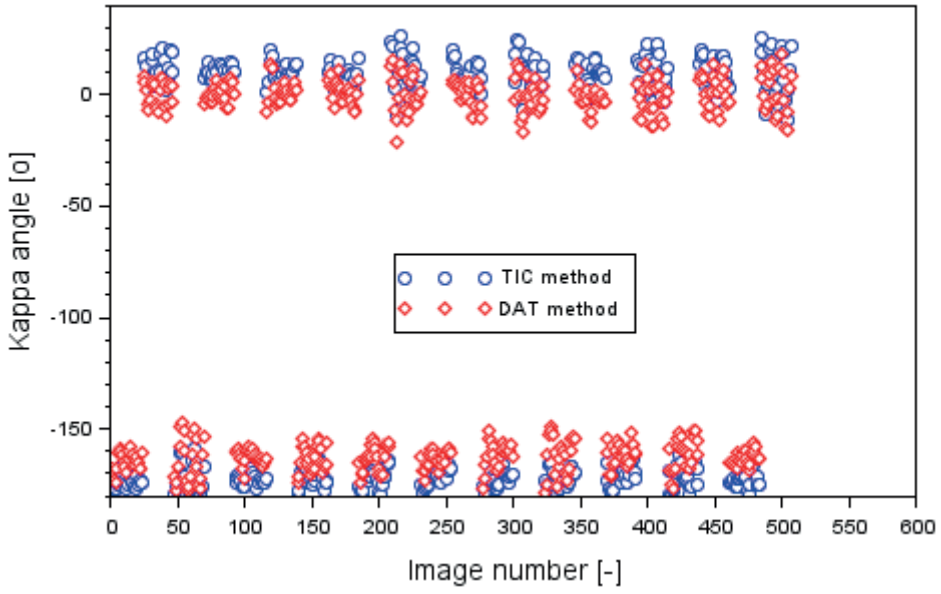

Figure 7 *Values of the Kappa angle based on TIC and DAT methods*

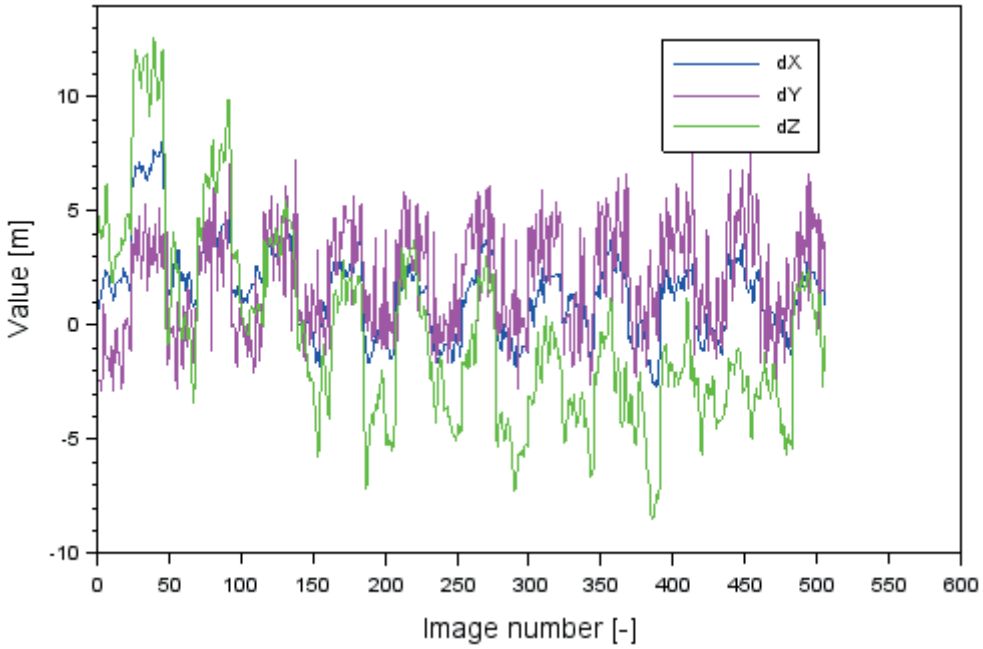

Figure 8 *Difference of projection centre coordinates based on TGC and DAT methods*

12.58 m. The standard deviation for parameter dZ equals 4.20 m, with the median being equal to -1.23 m. Among the calculated parameters dX, dY and dZ, the smallest dispersion (scatter) of results is noticeable for parameter dX. In addition, the dY parameter has the smallest standard values of deviation and of the median. Then, the largest scatter of results and standard deviation are visible for the value of the dZ parameter.

Figure 9 shows a difference in the exterior rotation angle elements on the example of the research methods TIC and DAT. The difference in the values of angle elements of exterior orientation was determined based on dependency [15]:

$$\begin{cases} d\varpi = \varpi^{TIC} - \varpi^{DAT} \\ d\varphi = \varphi^{TIC} - \varphi^{DAT} \\ d\kappa = \kappa^{TIC} - \kappa^{DAT} \end{cases}, \tag{6}$$

where:

$(\varpi^{TIC}, \varphi^{TIC}, \kappa^{TIC})$ - angular elements of the exterior orientation in the TIC solution,

$(\varpi^{TAD}, \varphi^{TAD}, \kappa^{TAD})$ - angular elements of the exterior orientation in the TAD solution.

The average value of parameter dω is equal to -0.07^0 with the scatter of results ranging from -15.40^0 to 14.05^0. Moreover, the standard value for parameter dω is 4.41^0 and the median is equal to -0.20^0. The average value of parameter dφ is equal to -0.33^0 with the scatter of results

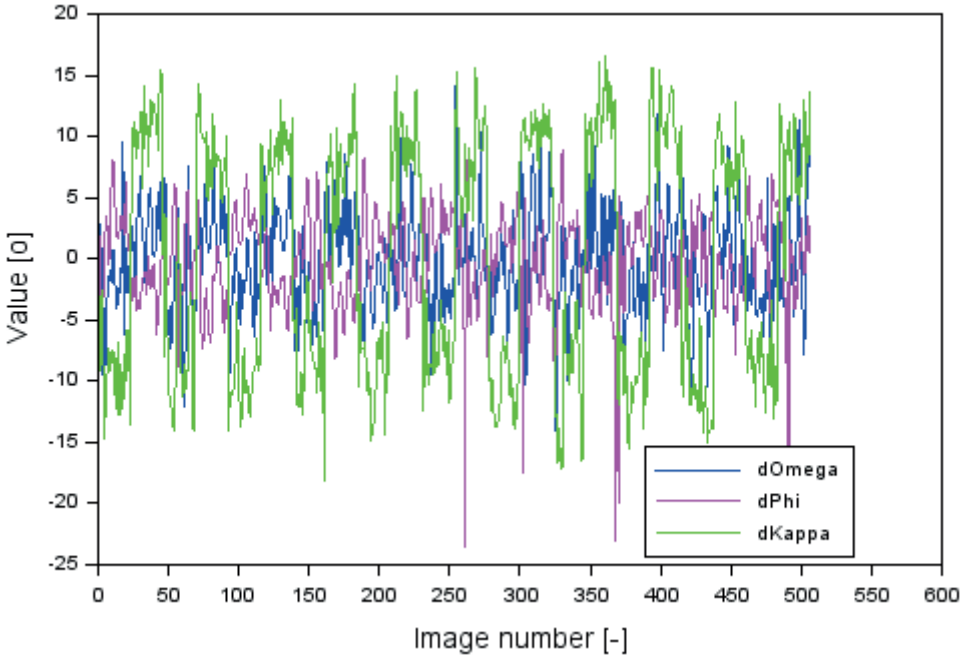

Figure 9 *Difference of the exterior orientation angle elements based on TIC and DAT methods*

ranging from -23.57^0 to 8.98^0. Moreover, the standard value for parameter dφ is 4.00^0 and of the median it is equal to -0.08^0. The average value of parameter dκ is equal to 0.06^0 with the scatter of results ranging from -18.23^0 to 16.64^0. Moreover, the standard value for parameter dκ is 9.86^0, and the median is equal to 2.15^0. The dω parameter has the smallest values of dispersion of the obtained findings, while the standard deviation and the median are the smallest for parameter dφ. The largest value of standard deviation and of the median are visible for parameter dκ.

5 Conclusions

The article describes and presents the results of exploiting three test methods for determining the elements of exterior orientation in photogrammetry for the needs of photogrammetry for aerospace applications. The paper used:

- the TGC method, which allows determining the linear elements of exterior orientation based on navigation data from the GNSS receiver, mounted on an unmanned aircraft system,
- the TIC method, which allows determining the angular elements of exterior orientation based on YPR parameters recorded by the INS sensor,
- the TAD method, which allows designating the linear and angular elements of exterior orientation in the model of digital aerial triangulation.

The research experiment was carried out for navigational data derived from the Trimble UX-5 rover. The photogrammetric flight was executed over Tylicz in 2016. During the flight, 506 images were taken at an altitude of 150 m. They were used in the process of digital aerial triangulation. For the needs of digital aerial triangulation, more than ten ground control points and five independent check points were measured. Based on the conducted investigations, it was found that:

- the calculated dY parameter has the smallest values of the median (e.g. 1.99 m) and of the standard deviation (e.g. 2.43 m),
- the calculated dZ parameter has the smallest values of the median (e.g. -0.38 m) and highest of the standard deviation (e.g. 4.30 m),
- the calculated dX parameter has the smallest value of the median (e.g. 1.48 m),
- the calculated dφ parameter has the smallest values of the median (e.g. -0.33^0) and of the standard deviation (e.g. 4.00^0),
- the calculated dκ parameter has the smallest values of the median (e.g. 0.06^0) and highest of the standard deviation (e.g. 9.86^0),
- the calculated dω parameter has the smallest dispersion of results with range between -15.40^0 to 14.05^0.

Acknowledgements

This paper was supported by Polish Air Force University and by the Military University of Technology, the Faculty of Civil Engineering and Geodesy, Institute of Geodesy.

References

[1] GINI, R., PAGLIARI, D., PASSONI, D., PINTO, L., SONA, G., DOSSO, P., BILL, R. UAV photogrammetry: block triangulation comparisons. *The International Archives of the Photogrammetry, Remote Sensing and Spatial Information Sciences* [online]. 2013, **XLI**(W2), p. 157-162. ISSN 1682-1750, eISSN 2194-9034. Available from: https://doi.org/10.5194/isprsarchives-XL-1-W2-157-2013

[2] COLOMINA, I., MOLINA, P. Unmanned aerial systems for photogrammetry and remote sensing: a review. *ISPRS Journal of Photogrammetry and Remote Sensing* [online]. 2014, **92**, p. 79-97. ISSN 0924-2716, eISSN 1872-8235. Available from: https://doi.org/10.1016/j.isprsjprs.2014.02.013

[3] RIEKE, M., FOERSTER, T., GEIPEL, J., PRINZ, T. High-precision positioning and real-time data processing of UAV systems. *International Archives of the Photogrammetry, Remote Sensing and Spatial Information Sciences* [online]. 2011, **38**(1/C22), p. 119-124. ISSN 1682-1750, eISSN 2194-9034. Available from: https://doi.org/10.5194/isprsarchives-XXXVIII-1-C22-119-2011

[4] GASPAROVIC, M. JURJEVIC, L. Gimbal influence on the stability of exterior orientation parameters of UAV acquired images. *Sensors* [online]. 2017, **17**(2), p. 401. eISSN 1424-8220. Available from: https://doi.org/10.3390/s17020401

[5] JIANG, S., JIANG, W., On-board GNSS/IMU assisted feature extraction and matching for oblique UAV images. *Remote Sensing* [online]. 2017, **9**, p. 813. eISSN 2072-4292. Available from: https://doi.org/10.3390/rs9080813

[6] IZOLTOVA, J., PISCA, P., CERNOTA, P., MANCOVIC, M., Adjustment of code ranging of GNSS observations. *Communications - Scientific Letters of the University of Zilina* [online]. 2016, **18**(4), p. 15-18. ISSN 1335-4205, eISSN 2585-7878. Available from: http://komunikacie.uniza.sk/index.php/communications/article/view/283

[7] SUN, Y., SUN, H., YAN, L., FAN, S., CHEN, R., RBA: Reduced bundle adjustment for oblique aerial photogrammetry. *ISPRS Journal of Photogrammetry and Remote Sensing* [online]. 2016, **121**, p. 128-142. ISSN 0924-2716, eISSN 1872-8235. Available from: https://doi.org/10.1016/j.isprsjprs.2016.09.005

[8] SCHNEIDER, J., LABE, T., FORSTNER, W. Incremental real-time bundle adjustment for multi-camera systems with points at infinity. *The International Archives of the Photogrammetry, Remote Sensing and Spatial Information Sciences* [online]. 2013, **XLI(**W2), p. 355-360. ISSN 1682-1750, eISSN 2194-9034. Available from: https://doi.org/10.5194/isprsarchives-XL-1-W2-355-2013

[9] BLAZQUEZ, M., COLOMINA, I. Relative INS/GNSS aerial control in integrated sensor orientation: models and performance. *ISPRS Journal of Photogrammetry and Remote Sensing* [online]. 2012, **67**, p. 120-133. ISSN 0924-2716, eISSN 1872-8235. Available from: https://doi.org/10.1016/j.isprsjprs.2011.11.003

[10] WIERZBICKI, D. Determine the position and attitude of UAV in air navigation based on GNSS data. 22nd International Conference Scientific Transport Means: proceedings. 2018. ISSN 1822-296X, eISSN 2351- 7034, p. 278-285.

[11] FORLANI, G., DIOTRI, F., MORRA DI CELLA, U., RONCELLA, R. Indirect UAV strip georeferencing by on-board GNSS data under poor satellite coverage. *Remote Sensing* [online]. 2019, **11**(15), p. 1765. eISSN 2072-4292. Available from: https://doi.org/10.3390/rs11151765

[12] WIERZBICKI, D. Determination of Shift/Bias in digital aerial triangulation of UAV imagery sequences. *IOP Conference Series: Earth and Environmental Science* [online]. 2017, **95**, 032033. ISSN 1755-1307, eISSN 1755-1315. Available from: https://doi.org/10.1088/1755-1315/95/3/032033

[13] WIERZBICKI, D. The prediction of position and orientation parameters of UAV for video imaging. *The International Archives of the Photogrammetry, Remote Sensing and Spatial Information Sciences* [online]. 2017, **XLII-2**(W6). ISSN 1682-1750, eISSN 2194-9034. Available from: https://doi.org/10.5194/isprs-archives-XLII-2-W6-407-2017

[14] WIERZBICKI, D., KRASUSKI, K. Determination the coordinates of the projection center in the digital aerial triangulation using data from unmanned aerial vehicle (in Polish). *Aparatura Badawcza i Dydaktyczna*. 2016, **21**, p. 127-134. ISSN 1426-9600.

[15] BURKER, M., HEIMES, F. J. *New* calibration and computing method for direct georeferencing of image and scanner data using the position and angular data of a hybrid inertial navigation system. OEEPE-Workshop Integrated Sensor Orientation: proceedings. 2001.

[16] YI Z., JIANG, G., YANAN D. Speed-up matching method with navigation data for UAV remote sensing images of coastal region. Remote Sensing of the Environment: 19th National Symposium on Remote Sensing of China: proceedings. 2015.

[17] RABAH, M., BASIOUNY, M., GHANEM, E., ELHADARY, A. Using RTK and VRS in direct geo-referencing of the UAV imagery. *NRIAG Journal of Astronomy and Geophysics* [online]. 2018, **7**(2), p. 220-226. eISSN 2090-9977. Available from: https://doi.org/10.1016/j.nrjag.2018.05.003

[18] GRUEN, A. Adaptive least squares correlation: a powerful image matching technique. *South African Journal of Photogrammetry Remote Sensing and Cartography*. 1985, **14**(3), p. 175-187. ISSN 0085-6398.

[19] WIERZBICKI, D. Estimation of angle elements of exterior orientation for UAV images based on ins data and aerial triangulation processing. 17th International Scientific Conference Engineering for Rural Development: proceedings [online]. 2018. ISSN 1691-5976, p. 1990-1996. Available from: https://doi.org/10.22616/ERDev2018.17.N054

Annex - Nomenclature of used abbreviations

Abbreviation	Full name
GNSS	Global Navigation Satellite System
UAVs	Unmanned Aerial Vehicles
INS	Inertial Navigation System
YPR	Yaw, Pitch and Roll
XYZ	Geocentric coordinates
GPS	Global Positioning System
OPK	Omega, Phi, Kappa
GCPs	ground control points
RTK	Real Time Kinematic
TGC	Translation between GPS sensor and Camera sensor
DAT	Digital Aerial Triangulation processing
PUWG2000	Local frame of Cartesian coordinates in Poland
RMS	Root Mean Square